0026-895X/04/6503-646–654$20.00
MOLECULAR PHARMACOLOGY
Copyright © 2004 The American Society for Pharmacology and Experimental Therapeutics
Mol Pharmacol 65:646–654, 2004

Vol. 65, No. 3
2781/1129860
Printed in U.S.A.

Selective Knock-Down of $P2X_7$ ATP Receptor Function by Dominant-Negative Subunits

Ramin Raouf, Yassar Chakfe, Dominique Blais, Audrey Speelman, Eric Boué-Grabot, Duncan Henderson, and Philippe Séguéla

Montreal Neurological Institute, Department of Neurology and Neurosurgery, McGill University, Montreal, Quebec, Canada (R.R., Y.C., D.B., A.S., P.S.); Unité Mixte de Recherche 5543, Centre National de la Recherche Scientifique, Université Victor Segalen Bordeaux 2, Bordeaux, France (E.B.-G.); and AstraZeneca R&D Charnwood, Loughborough, England (D.H.)

Received July 1, 2003; accepted November 21, 2003

This article is available online at http://molpharm.aspetjournals.org

ABSTRACT

Among the family of P2X ATP-gated cation channels, the $P2X_7$ receptor is a homomeric subtype highly expressed in immune cells of the monocyte-macrophage lineage. We report here that the WC167–168AA mutation in the ectodomain of $P2X_7$ produced nonfunctional subunits with strong dominant-negative effect on wild-type $P2X_7$ receptors (77% inhibition with cotransfection of wild-type and mutant DNA at a ratio of 3:1). The C168A single mutant was also very effective in suppressing $P2X_7$ receptor function (72% reduction at a DNA ratio of 3:1), indicating the major role played by the C168A mutation in this inhibition. The dominant-negative effect is selective; the mutant subunit did not suppress the function of other receptor-channel subtypes. The reduced current responses in cells coexpressing wild-type and dominant-negative subunits display wild-type characteristics in both agonist affinity and ionic selectivity, strongly suggesting that the heteromeric channels are functionally impaired. The mutant subunits also suppressed the $P2X_7$-dependent pore formation as assessed by uptake of the propidium dye YO-PRO-1 (Molecular Probes, Eugene, OR) in response to 2′,3′-*O*-(4-benzoyl)-benzoyl-ATP (BzATP) in transfected human embryonic kidney 293 cells. Native responses to BzATP as well as ATP-induced ethidium dye uptake were significantly knocked down (31 ± 9% and 25 ± 7% of control, respectively) in mouse macrophage cell line RAW264.7 transfected with the mutant subunits. Therefore, these dominant-negative subunits provide selective genetic tools to investigate the functional roles of native $P2X_7$ receptors.

Ionotropic P2X receptors constitute a family of calcium-permeable nonselective cation channels gated by extracellular ATP. Their primary structures define a unique class of multimeric ion channels composed of subunits with two transmembrane domains connected by a large ectodomain. Seven genes coding for P2X channel subunits have been cloned in mammals, and their functional characterization has been described in recombinant systems in homomeric and/or heteromeric forms as well as in native systems (for review, see North, 2002). The $P2X_7$ receptor is a homomeric subtype highly expressed in immune cells of the monocyte-macrophage lineage, including microglial and dendritic cells (Collo et al., 1997). One distinct structural feature of $P2X_7$ receptor-channels, a large intracellular carboxyl-terminal domain (239 amino acids in mammalian subunits), is involved in the progressive formation of large pores permeable to molecules up to 900 Da (Surprenant et al., 1996; Virginio et al., 1999b) as well as in the efficient release of the pro-inflammatory cytokine interleukin 1-β, as demonstrated in a knock-out model (Solle et al., 2001). In macrophage-related cells and glia, ATP-induced $P2X_7$ activity has been reported to be linked to a number of cellular events including membrane blebbing and microvesiculation (Virginio et al., 1999a; MacKenzie et al., 2001), cell fusion (Chiozzi et al., 1997), activation of nuclear factor-κB and nuclear factor of activated T cells (Ferrari et al., 1997, 1999), activation of p38 mitogen-activated protein kinase (Neary et al., 2003), activation of phospholipase D (Dubyak and el-Moatassim, 1993; el-Moatassim and Dubyak, 1993), killing of intracellular mycobacteria (Lammas et al., 1997; Smith et al., 2001), and cell death (Di Virgilio et al., 1998). Although it is not known whether these cellular events depend on specific functional properties of the $P2X_7$ subtype, they underline the significant

This work was supported by an operating grant from the Canadian Institutes of Health Research (CIHR) and by AstraZeneca Charnwood. R.R. is supported by the Pain: Molecules to Community CIHR Strategic Training Program. Y.C. was a recipient of a fellowship from the Savoy Foundation. P.S. is a Scholar of the Fonds de la Recherche en Santé du Québec.

R.R. and Y.C. contributed equally to this work.

This work was presented in part at the 32nd Annual Meeting of Society for Neuroscience; 2002 Nov 2–7; Orlando, Florida.

ABBREVIATIONS: BzATP, 2′,3′-*O*-(4-benzoyl)-benzoyl-ATP; KN-62, 1-[*N*,*O*-bis-(5-isoquinolinesulfonyl)-*N*-methyl-L-tyrosyl]-4-phenylpiperazine; HEK, human embryonic kidney; GFP, green fluorescent protein.

role played by $P2X_7$ receptors in the regulation of immune response in peripheral tissues as well as in the central nervous system. Despite the potential physiological and therapeutic importance of $P2X_7$ receptors, their pharmacology remains limited. The agonist 2′,3′-*O*-(4-benzoyl)-benzoyl-ATP (BzATP) is more potent than ATP at activating rodent and human $P2X_7$ receptors, and this marked difference in sensitivity has been naturally used as an index of the presence of native $P2X_7$ receptors. However, their identification cannot be based solely on this differential sensitivity because BzATP has been reported to be an agonist for other P2X receptor subtypes (Bianchi et al., 1999; Boué-Grabot et al., 2000a). Irreversible blockade of P2X responses by long incubations with oxidized ATP was also considered a solid proof of the involvement of native $P2X_7$ receptors; however, oxidized ATP has subsequently been shown to block P2X1 and P2X2 receptors (Evans et al., 1995). A monoclonal antibody directed against an extracellular epitope of $P2X_7$ subunit has antagonistic properties, but its use is limited to human $P2X_7$ (Buell et al., 1998). In search of better antagonists, the dye Brilliant Blue G has been identified as a potent blocker of rat $P2X_7$ in the 10 to 100 nM range, but it blocks other subtypes in the micromolar range (Jiang et al., 2000a) and its actions on metabotropic ATP receptors have not been tested. The organic cation calmidazolium, a calmodulin antagonist and a blocker of cyclic nucleotide-gated channels (Virginio et al., 1997), is effective at blocking rat and human $P2X_7$ receptors but does not block pore formation (Chessell et al., 1998). Another $P2X_7$ antagonist, KN-62, a known inhibitor of calcium/calmodulin-dependent protein kinase type II, has little inhibitory effect on the rat $P2X_7$ (Humphreys et al., 1998). The lack of unambiguous and cross-species pharmacological tools for $P2X_7$ prompted us to develop specific sequence-based antagonists. We report here the characterization of dominant-negative mutations located in the ectodomain of $P2X_7$ subunits that are highly effective at selectively suppressing the function of rodent as well as human $P2X_7$ receptors. Moreover, we show that these dominant-negative $P2X_7$ subunits have the property of knocking down the activity of native $P2X_7$ receptor channels in immune cells.

Materials and Methods

Clones and Mutants. Rat $P2X_7$ subunit was cloned using reverse transcription-polymerase chain reaction; mouse and human $P2X_7$ subunits were isolated by screening brain cDNA libraries. Rat $P2X_2$ and mouse $5HT_{3A}$ subunits were kindly provided by D. Julius (University of California, San Francisco). Single and double mutants of mouse $P2X_7$ were generated using the QuikChange method (Stratagene, La Jolla, CA). The C-terminally tagged versions of wild-type and mutant $P2X_7$ cDNAs were constructed by removing the stop codons and subcloning a cassette encoding a FLAG epitope, according to previously published protocols (Boué-Grabot et al., 2000b).

Cell Culture and Transfections. HEK293 cells were cultured as described previously (Le et al., 1998). HEK293 cells stably expressing the rat $P2X_7$ subunit (HEK-$P2X_7$), kindly provided by A. Surprenant (University of Sheffield, Sheffield, England), were cultured in Dulbecco's modified Eagle's medium and 10% heat-inactivated fetal bovine serum (Invitrogen, Carlsbad ,CA) containing penicillin and streptomycin supplemented with G-418 (250 μg/ml). RAW264.7 cells were kindly provided by M. Desjardins (University of Montreal, PQ, Canada) and were cultured in Dulbecco's modified Eagle's medium and 10% heat-inactivated fetal bovine serum containing 10 mM HEPES buffer (Sigma, St. Louis, MO), 5% L-glutamine (Invitrogen), penicillin, and streptomycin. Cells were transfected with Polyfect (QIAGEN, Valencia, CA) or Fugene 6 (Roche Diagnostics, Indianapolis, IN) according to the manufacturer's protocols. Transfected cells were used for electrophysiological recordings 24 to 48 h after transfection. Oocytes were surgically removed from Tricaine-anesthetized female *Xenopus laevis* frogs and were incubated with calcium-free Barth's solution containing 1 mg/ml type I collagenase at room temperature for 2 h under vigorous agitation. Stage V and VI oocytes were then manually defolliculated before intranuclear microinjection of 1 to 10 ng of supercoiled plasmid coding for wild-type/mutant mouse $P2X_7$, human $P2X_7$, rat $P2X_7$ and $P2X_2$, or mouse $5HT_{3A}$. After injection, oocytes were incubated with Barth's solution containing 1.8 mM $CaCl_2$ at 19°C for 24 to 72 h before electrophysiological recordings.

Electrophysiology. Two-electrode voltage-clamp recordings (V_H = −60 mV) were performed using glass pipettes (1–3 MΩ) filled with 3 M KCl solution. Oocytes were placed in a recording chamber and were perfused at a flow rate of 10 to 12 ml/min with Ringer's solution, pH 7.4, containing 115 mM NaCl, 5 mM NaOH, 2.5 mM KCl, 1.8 mM $CaCl_2$, and 10 mM HEPES. Membrane currents (d.c., 1 kHz) were recorded using a Warner OC-725B amplifier (Warner Instrument, Hamden, CT) and digitized at 500 Hz. Drugs were dissolved in the perfusion solution and applied using a computer-driven valve system. Whole-cell patch-clamp recordings (V_H of −60 mV) were performed using pipettes filled with internal solution, pH 7.2, containing 120 mM K-gluconate, 1 mM $MgCl_2$, 4 mM NaOH, and 10 mM HEPES. Drugs were applied using a Warner SF-77B fast perfusion system at a rate of 1 ml/min. The perfusion solution, pH 7.4, comprised 145 mM NaCl, 5 mM NaOH, 3 mM KCl, 1 mM $MgCl_2$, 0.9 mM $CaCl_2$, and 10 mM HEPES. Membrane currents (d.c., 200 Hz) were recorded using an Axopatch 200B amplifier (Axon Instruments Inc., Union City, CA) and digitized at 500 Hz. All drugs were dissolved in the perfusion solution. Current-voltage plots were obtained using a ramp protocol. All experiments were performed at room temperature.

YO-PRO-1 and Ethidium Uptake Imaging. The BzATP-dependent $P2X_7$ mediated pore formation was assessed by imaging the uptake of YO-PRO-1 (Molecular Probes, Eugene, OR), a 629-Da propidium di-iodide dye that fluoresces when bound to nucleic acids. HEK293 cells were cotransfected with CD8 and wild-type or mutant $P2X_7$ subunits. Twenty-four hours after transfection, dishes were rinsed twice with perfusion solution and incubated with 2×10^7 beads/ml of Dynabeads (Dynal Biotech, Lake Success, NY) for 30 min. After washing, the cells were incubated with perfusion solution containing 1 μM YO-PRO-1. BzATP (300 μM) was dissolved in low divalent solution, pH 7.4, containing 145 mM NaCl, 5 mM NaOH, 3 mM KCl, 0.09 mM $CaCl_2$, and 10 mM HEPES. Fluorescence changes (excitation, 491 nm; emission, 509 nm) were monitored in individual cells rosetted by the beads. RAW264.7 cells were transfected with mutant subunit subcloned in pAdTrack vector containing a GFP expression cassette. After transfection (24 to 48 h), GFP-positive cells were monitored for changes in ethidium fluorescence signals (excitation, 525 nm; emission, 565 nm) in response to application of low divalent solution containing 10 μg/ml ethidium bromide in the presence or absence (control) of 3 mM ATP, pH 7.4. The fluorescence signals were corrected for baseline signal levels in control experiments. Images were captured every 30 s on a cooled charge-coupled device camera (Optikon, Kitchener, ON, Canada) and processed using Axon Imaging Workbench 2.2 software (Axon Instruments).

Immunocytochemistry and Confocal Microscopy. Transiently transfected HEK293 cells were fixed with 4% paraformaldehyde (Electron Microscopy Sciences, Hatfield, PA) in 0.16 M phosphate buffer, pH 6.8. The cells were washed and blocked with 5% normal goat serum (Jackson ImmunoResearch Laboratories Inc., West Grove, PA), 0.3% Triton X-100 (Fisher Scientific, Pittsburgh, PA) in phosphate-buffered saline, pH 7.4, then incubated with anti-FLAG M2 antibody (Sigma) at 4°C overnight. Antibody binding was then revealed using a Texas Red conjugated goat anti mouse (Jack-

son ImmunoResearch) for 60 min at room temperature. The confocal fluorescence microscopy images were acquired using an LSM 510 line scanning microscope (Zeiss, Jena, Germany).

Data Analysis. Peak currents, defined as the largest amplitudes recorded during agonist applications, were normalized to the mean of the wild-type currents under each experimental condition. Data are presented as mean ± S.E. The BzATP EC_{50} values were calculated by fitting the data to logistical equation using Sigmaplot software (SPSS Inc., Chicago, IL). The proportions of homomeric and heteromeric channels were calculated using binomial distribution. Assuming that heteromeric channels composed of one or more mutant subunits are silent, then the fraction of total current (I/I_{Total}) is obtained using the binomial equation $I/I_{Total} = (1 - p)^n$ where p is the proportion of mutant subunits and n is the number of subunits in the channel complex. All statistical analyses for the difference in means were carried out using Student's t tests for two unpaired groups. The analysis for the immunofluorescence intensity profiles was carried out using ImageJ software (http://rsb.info.nih.gov/ij).

Results

Mutagenesis and Functional Screening. We reasoned that conserved residues among $P2X_7$ receptors from different species that are also present in other P2X subtypes may prove critical for their function. We engineered a number of mutant rat $P2X_7$ subunits and screened them, using two-electrode voltage-clamp recordings, for their response to BzATP and for their dominant-negative effect when coexpressed with the wild-type subunit in *X. laevis* oocytes. As summarized in Table 1 and illustrated in Fig. 1, we observed three phenotypes: 1) functional mutants that produced a current response when expressed alone and did not inhibit the wild-type current when coexpressed (e.g., Y13A; Fig. 1A); 2) nonfunctional mutants that did not inhibit the wild-type current when coexpressed (e.g., DI316–317AA; Fig. 1B); and 3) a nonfunctional mutant that had a dominant-negative effect on wild-type current (WC167–168AA; Fig. 1C). Because the motif WC167–168 is conserved in all mammalian $P2X_7$ subunits, we investigated whether the WC167–168AA mutation in mouse $P2X_7$ subunit has a dominant-negative effect and can block human $P2X_7$ receptors. We therefore conducted whole-cell voltage-clamp recordings from HEK293 cells transfected with wild-type, mutant, or both at a ratio of 1:1. As shown in Fig. 2, coexpression of WC167–168AA subunit with wild-type subunits significantly decreased BzATP-evoked currents mediated by mouse (Fig. 2A; 14 ± 2% of wild-type current, $n = 10$; $p < 0.01$) and human $P2X_7$ receptors (Fig. 2B; 23 ± 4% of wild-type current; $n = 8$, $p < 0.01$). However, the WC167–168AA mutant inhibited neither ATP-induced currents in cells cotransfected with $P2X_2$ (Fig. 2C) nor serotonin-evoked currents in cells cotransfected with unrelated $5HT_{3A}$ receptor (Fig. 2D). The WC167–168AA mutation, therefore, has a selective dominant-negative effect on rodent and human $P2X_7$ receptors.

WC167–168AA Mutant Inhibits YO-PRO-1 Uptake. Activation of $P2X_7$ receptors results in opening of nonspecific pores permeable to molecules smaller than 900 Da, such as YO-PRO-1 (Surprenant et al., 1996). We investigated whether the WC167–168AA mutant subunit can block $P2X_7$-mediated permeabilization. As shown in Fig. 3, A and B, control cells transfected with the nonfluorescent marker CD8 alone showed no significant increase in YO-PRO-1 uptake in response to BzATP. Cells transfected with wild-type $P2X_7$ showed a marked time-dependent increase in YO-PRO-1 uptake upon stimulation with BzATP, whereas cells cotransfected with the WC167–168AA mutant and the wild-type subunits (1:1 ratio) exhibited a significantly decreased YO-PRO-1 uptake in response to agonist (12 ± 2% of the $P2X_7$ transfected cells, 20 min after BzATP application, $n = 4$).

Impact of WC167–168AA Mutant on Receptor-Channel Properties. To determine whether the expression of the mutant causes a decrease in the agonist sensitivity, we obtained the dose-response curves for BzATP in cells transfected with $P2X_7$ alone or in the presence of the WC167–168AA mutant (at a 2:1 ratio). As illustrated in Fig. 4A, at any given concentration, the magnitude of current in the cotransfection was smaller than the wild-type. The dose-responses exhibited a sigmoidal relationship with an EC_{50} of 538 ± 75 μM for the wild-type and 556 ± 31 μM for the cotransfection ($n = 4$) (Fig. 4B). To investigate whether the coexpression of the mutant subunit changed the ionic selectivity of $P2X_7$ receptor-channels, we plotted the current-voltage (I-V) relationship for BzATP-evoked currents in cells transfected with wild-type subunit alone or cotransfected with the WC167–168AA subunit. In both cases, I-V relationship displayed a linear slope between −70 and +30 mV. Moreover, as shown in Fig. 4C, the reversal potential of BzATP-evoked currents in cells transfected with wild-type alone was not significantly different from that obtained in cells cotransfected with the WC167–168AA subunit (1.3 ± 2.6 mV versus −1.3 ± 1.7 mV; respectively, $n = 5$). These results indicate that the WC167–168AA mutant does not inhibit $P2X_7$ receptor-channels function by reducing agonist

TABLE 1

Functional screening of mutant $P2X_7$ subunits

Single and double mutations in rat $P2X_7$ subunit were designed to target residues conserved in the mammalian P2X family. The mutant receptors were assayed for their response to 50 μM BzATP. The dominant-negative (Dn) effect of the mutant subunits was determined at a 2:1 ratio with the wild-type subunit.

Motif	Domain	Mutation	Response to BzATP	Dn Effect
D V F Q Y E T N K	Intracellular	Y13A	+	−
F Q Y E T N K V T	Intracellular	T15A	+	−
I/T V F S Y I/V S F A	Transmembrane	Y40A	+	−
V/I S/F A W C P T/A E E	Extracellular	WC167–168AA	−	+
Y W D C N L D S W	Extracellular	CN260–261AA	−	−
I K A F G I/V R F D	Extracellular	FG313–314AA	+	−
F G I/V R F D I L V	Extracellular	RF316–317AA	−	−
I/V R F D I L V F G	Extracellular	DI318–319AA	−	−
G T G B G K F D I T	Extracellular	GK326–327AA	+	−
Q L V V Y I G S T	Transmembrane	Y336A	+	−
V Y I G S T L S Y	Transmembrane	S339R	+	−
T VC I D L L/I I N	Transmembrane	D352A	+	−

sensitivity or by changing the relative permeability of sodium and potassium ions.

Subcellular Localization of the WC167–168AA Mutant Subunit. To assess the subcellular distribution of the WC167–168AA subunit, we immunolocalized FLAG epitope-tagged versions of wild-type or mutant receptors in HEK293 cells. The profiles of the receptor distributions, obtained by measuring the fluorescence intensity along a line randomly drawn through the diameter of the cell, were identical for both the wild-type and mutant subunits (Fig. 5, A–C). The staining for wild-type and mutant $P2X_7$ subunits was most intense at the edges of the cell, in contrast to the cytoplasmic

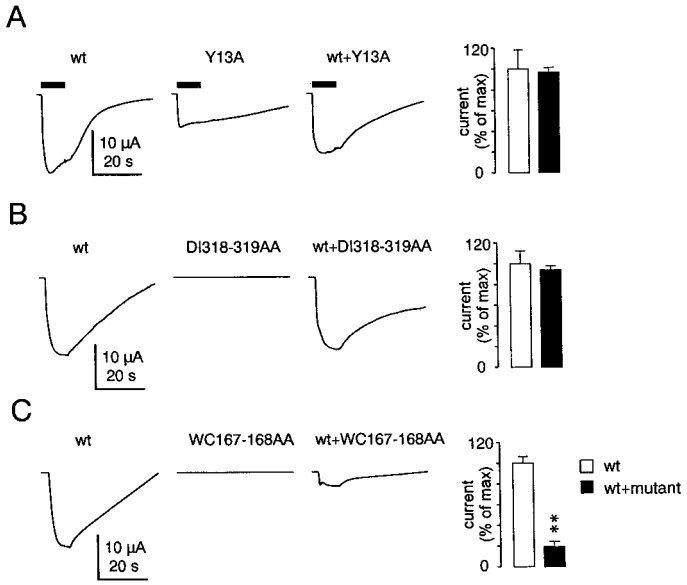

Fig. 1. Representative phenotypes of mutant P2X7 subunits. A, a functional mutant (Y13A) giving a weaker response to BzATP without any inhibitory effects on wild-type $P2X_7$ receptors. B, a silent mutant (DI318–319AA) with no inhibitory effect on wild-type $P2X_7$ receptors. C, the WC167–168AA mutant is silent and exhibits a dominant-negative effect on wild-type $P2X_7$ receptors (20 ± 5% of wild-type current, $n = 5$, $p < 0.01$). Voltage-clamp recordings were carried out in *Xenopus* oocytes. Wild-type to mutant cDNA ratio was 1:2.

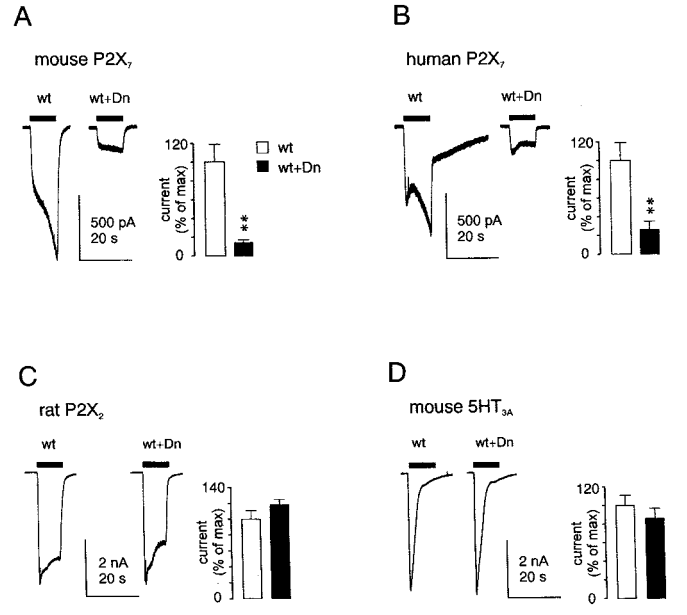

Fig. 2. Dominant-negative mutant subunits selectively suppress $P2X_7$ channel activity. A and B, at a 1:1 ratio, mouse WC167–168AA $P2X_7$ subunit (Dn) strongly suppressed BzATP-induced responses mediated by both wild-type mouse (14 ± 2% of control, $p < 0.01$, A) and human $P2X_7$ receptors (23 ± 4% of control, $p < 0.01$, B). C and D. The mutant did not interfere with the function of $P2X_2$ or unrelated $5HT_{3A}$ receptors when coexpressed. Wild-type to mutant cDNA ratio was 1:1.

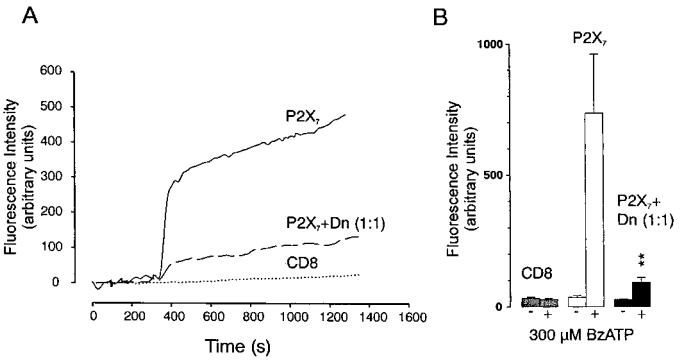

Fig. 3. Suppression of YO-PRO-1 uptake by dominant-negative subunits. A, time-dependent increase in fluorescence intensity in response to application of 300 μM BzATP in low divalent extracellular solution is shown. HEK293 cells were transfected with wild-type $P2X_7$ subunits or cotransfected with WC167–168AA and wild-type $P2X_7$ subunits ($P2X_7$ + Dn) or transfected with CD8 only. Agonist was applied at time 300 s. B. The average YO-PRO-1 fluorescence intensities in the presence (+) or absence (−) of BzATP stimulation. The YO-PRO-1 uptake in cells coexpressing the wild-type and mutant subunits is lower than in cells expressing wild-type subunit alone (89 ± 17 versus 736 ± 225 arbitrary units, $n = 4$, $p < 0.01$).

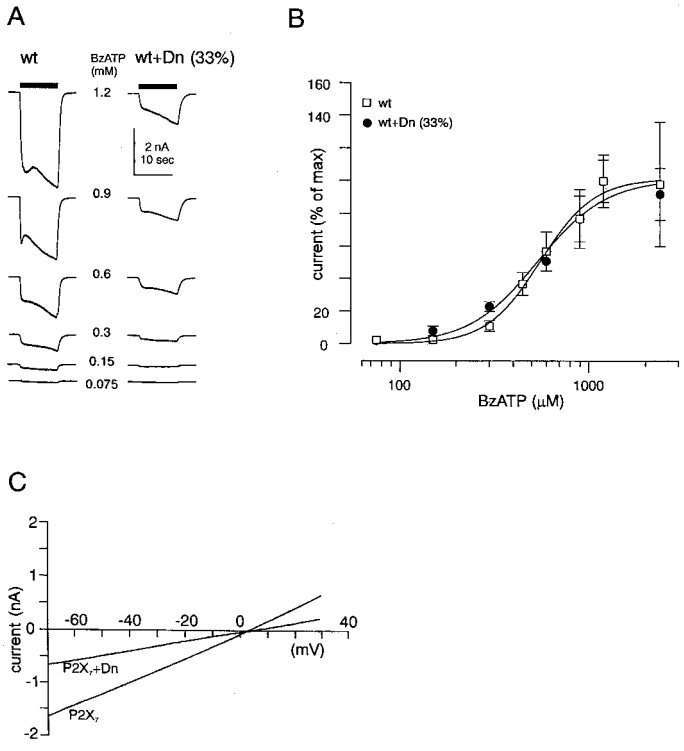

Fig. 4. Receptor-channel properties in cells coexpressing wild-type and WC167–168AA subunits A. Representative recordings of whole cell $P2X_7$ currents at different concentrations of BzATP in HEK293 cells expressing wild-type $P2X_7$ alone or in combination with WC167–168AA subunit (Dn) at a 2:1 ratio. Note the suppression of current at all concentrations of BzATP tested. B, no significant decrease in the EC_{50} values for BzATP between $P2X_7$ and ($P2X_7$ + Dn) currents. C, current-voltage relationship for BzATP currents in cells expressing $P2X_7$ alone or with Dn. The slope conductance is linear at holding potentials between −70 and +30 mV. No significant change in the current reversal potential was observed in the presence of Dn (+1.3 ± 2.6 versus −1.3 ± 1.7 mV for wild-type alone, $n = 4$).

distribution of EGFP in the same cell (Fig. 5D). These results show that most wild-type and mutant subunits are transported to the plasma membrane, hence indicating that the functional knock-down of P2X7 receptor is not caused by disturbed trafficking or intracellular retention.

Potency of Inhibitory WC167–168AA and C168A Mutants. To determine the potency of the inhibitory effect of the WC167–168AA subunits on $P2X_7$ receptors, HEK293 cells were transfected with a fixed concentration of wild-type cDNA and varying concentrations of the mutant. As illustrated in Fig. 6A, the amplitude of the current is greatly reduced (74 ± 6%) by cotransfecting wild type with mutant subunits at a ratio as low as 2:1. The amplitude of BzATP-evoked currents decreased with increasing proportions of the mutant subunit, as expected for a dominant-negative effect (Fig. 6C and Table 2).

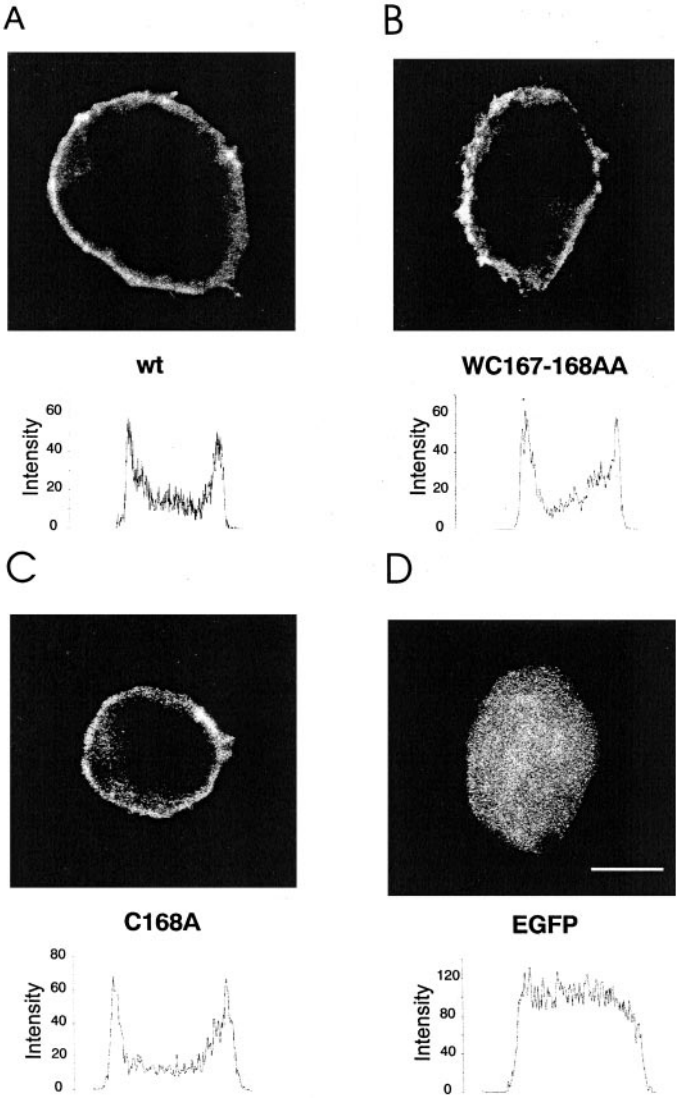

Fig. 5. Subcellular distribution of wild-type and mutant $P2X_7$ subunits. A, representative immunolocalization of wild-type mouse $P2X_7$ tagged with FLAG epitope. The intensity of staining is highest at the edges of the cell (lower). B and C, representative examples of the distribution of FLAG-tagged WC167–168AA and C168A mutants in HEK293 cells. D, cytoplasmic distribution of EGFP protein in the same cell as in B. Scale bar (5 μm) applies to all images and intensity profiles.

Next, we sought to determine the key residue involved in the inhibitory effect of the WC167–168AA subunit. We investigated the effects of single W167A and C168A mutations on the function of the $P2X_7$ receptor. The W167A mutant was nonfunctional when expressed alone, with no obvious dominant-negative effects (data not shown). The C168A mutant, on the other hand, exhibited a substantial inhibitory effect as shown in Fig. 6B (80 ± 5% at 2:1 ratio). The dominant-negative effect increased exponentially with increasing proportions of mutant subunit (Fig. 6C and Table 2). These data indicate that the WC167–168AA and C168A mutants are highly effective inhibitory subunits for $P2X_7$ receptors.

Knock-Down of Native $P2X_7$ Function by Dominant-Negative Mutants. In the previous experiments, we assessed the knock-down of wild-type receptors transiently co-expressed with the mutant subunits in heterologous systems. However, in cells natively expressing $P2X_7$ receptors, there is a pre-existing pool of surface receptors. So, as a first step to test the sensitivity of endogenous $P2X_7$ receptors to dominant-negative blockade, we investigated the effect of the

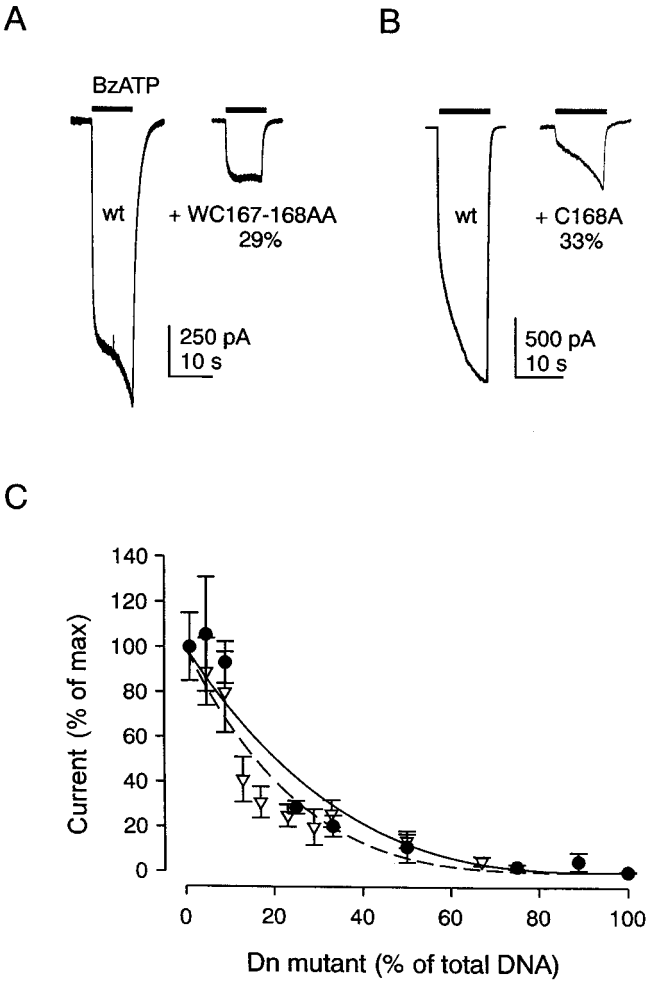

Fig. 6. Dose dependence of the inhibitory effects of WC167–168AA and C168A mutants on wild-type receptors. A and B, typical examples of current responses to application of 700 μM BzATP in the presence or absence of the mutant subunits. C, dose-response relationship for the dominant-negative effects of WC167–168AA (▽) and C168A (●) mutants. HEK293 cells were transfected with a fixed concentration of wild-type P2X7 cDNA and varying concentrations of the mutant subunits. The solid and dashed lines represent the expected dose-response curves assuming trimeric and tetrameric channel configuration, respectively.

expression of the mutant subunits in HEK293 cells stably expressing $P2X_7$ receptors (HEK-$P2X_7$) at a high level (Surprenant et al., 1996). In HEK-$P2X_7$ cells, transient expression of the WC167–168AA mutant subunits resulted in a significant reduction of the current responses to BzATP (15 ± 5% of control, $p < 0.05$, $n = 3$, Fig. 7A). Next, we tested the effects of expression of the dominant-negative subunits in mouse macrophage cell line RAW264.7. As shown in Fig. 7B, the dominant-negative C168A subunit significantly reduced the endogenous current responses to BzATP (31 ± 9% of control, $p < 0.05$, $n = 3$, Fig. 7B). Pore formation measured by the uptake of ethidium ions in response to application of agonist was also knocked down by transient expression of the C168A mutant subunit (25 ± 7% of control, $p < 0.01$, Fig. 8). These results indicate that the C168A dominant-negative subunits are able to effectively suppress both the current response and pore formation mediated by native $P2X_7$ receptors in immune cells.

Discussion

In an effort to design pan-specific and subtype-selective inhibitors of mammalian $P2X_7$ ATP receptors, we searched for mutations with dominant-negative effect. The functional screening based on electrophysiological recordings led to the identification of one mutation with the required properties. The inhibitory $P2X_7$ subunit with double mutation WC167–168AA located in the ectodomain assembles into nonfunctional homomeric channels. Neither Trp167 nor Cys168, which are conserved in the whole P2X family, has been reported to be a determinant of the ATP-binding site (Jiang et al., 2000b). However, because of the presence of disulfide bridges in the ectodomain (Clyne et al., 2002; Ennion and Evans, 2002), the role of different extracellular regions in receptor function remains difficult to assess in the absence of crystallographic data. Nevertheless, we can conclude from this screening that the conserved P2X motif WC167–168 is not involved in subunit association. In our screen, the other nonfunctional subunits with mutations in the ectodomain displayed no inhibitory activity, suggesting either that they were degraded prematurely because of misfolding or that they did not associate correctly with the wild-type subunits.

Mammalian $P2X_7$ subunits share significant homology (e.g., 80% between mouse and human), so we hypothesized that they would be able to associate into hybrid receptor-channels. We confirmed the coassembly of mouse and human $P2X_7$ subunits by knocking down human $P2X_7$ receptor function with mouse WC167–168AA mutant subunits (Fig. 2). The logical consequence of this compatibility of association is that dominant-negative $P2X_7$ subunits from one species are able to suppress the function of $P2X_7$ receptors in other species. Therefore, this genetic approach based on the expression of mutant subunits provides an advantage over knockout strategies, which are currently limited to mice. Potentially, a gene therapy approach leading to the overexpression of dominant-negative $P2X_7$ subunits and the knockdown of human macrophage or microglial $P2X_7$ responses could be beneficial in the control of inflammatory diseases (Cucchiarini et al., 2003).

Phylogenetically and functionally, vertebrate $P2X_7$ subunits define a distinct gene subfamily (North, 2002). Indeed all P2X subunits have been shown to associate in heteromeric receptors (Khakh et al., 2001), except $P2X_7$ subunits, which seem to form homomers exclusively (Torres et al., 1999). This unique property of $P2X_7$ subunits provides a methodological advantage to selectively target the $P2X_7$ receptors while sparing all other coexpressed P2X subtypes. By coexpressing the mutant $P2X_7$ subunits with $P2X_2$ subunits, we demonstrated the subtype selectivity and we confirmed the absence of heteromeric $P2X_{2+7}$ ATP receptors. Likewise, the mutant $P2X_7$ subunit did not suppress the function of unrelated homomeric $5HT_{3A}$ receptor channels, chosen here as a prototypical member of the Cys-loop family of transmitter-gated channels. So, the WC167–168AA mutation conferred strong and specific dominant-negative effect to the subunit for the rodent and human $P2X_7$ subtypes of ionotropic ATP receptors.

Several members of the P2X receptor family, including $P2X_7$, are capable of forming large pores in response to agonist stimulation. The exact function of these pores is not known; however; given their ability to provide passage for molecules such as L-glutamate (Ballerini et al., 1996; Duan et al., 2003), they potentially play a crucial role in cell signaling and metabolism. The mechanisms linking channel activity and pore formation are not well understood. Calmidazolium has been shown to distinguish between the pore and channel states of $P2X_7$ receptors because it can block the channel without affecting the pore formation (Virginio et al., 1997). This suggests that the pore-forming activity of $P2X_7$ receptors may not require the opening of the channel. Given that other members of the P2X receptor family have been shown to promote pore formation (Khakh et al., 1999; Virginio et al.,

TABLE 2

The effect of co-expression of mutant and wild type subunits on current amplitude

The percentage of predicted total currents was calculated based on the binomial distribution of homomeric and heteromeric populations of channels in co-expression experiments. Incorporation of one mutant subunit was assumed to be sufficient to knock down the channel function.

DNA Ratio Wild-Type:Dn	Predicted Total Current			Observed Total Current	
	Stoichiometry			C168A	WC167–168AA
	Dimer	Trimer	Tetramer		
	%			%	
1: 0	100	100	100	100	100
1: 0.33	56.2	42.2	31.6	28.7 ± 2.9	22.6 ± 5.0
1: 0.5	44.4	29.5	19.7	20.40 ± 5.0	25.96 ± 6.0
1: 1	25	12.5	6.2	11.30 ± 7.0	14 ± 3.0
1: 3	6.2	1.6	0.4	2.5 ± 1.0	3.8 ± 3.0
0: 1	0	0	0	N.D.	N.D.

N.D., not detectable.

1999b), an effective tool for the study of $P2X_7$ receptors should also be able to block this function. Our YO-PRO-1 and ethidium uptake data demonstrate that the knock-down by the dominant-negative subunits is complete in that it suppresses both the channel- and the pore-forming functions of recombinant and native $P2X_7$ receptors.

Two mechanisms by which a dominant-negative subunit is likely to exert its inhibitory effect are either by binding and sequestering the agonist away from the receptor (sink effect) or by directly associating with the receptor and blocking its function. It seems unlikely that the dominant-negative subunits described here act via a sink effect because 1) mutation of the conserved cysteines in the ectodomain of other P2X receptors has been shown to reduce the sensitivity of the receptor to ATP (Clyne et al., 2002; Ennion and Evans, 2002) and 2) the dominant-negative subunits are highly effective at blocking the wild-type receptors at low proportions. Our data show that the reduced current response has wild-type characteristics in both agonist affinity and reversal potential, indicating that channels composed of dominant-negative and wild-type subunits are silent. Hence, the dominant-negative subunits probably block the function of $P2X_7$ receptors by association, which leads to a reduction in the number of homomeric wild-type channels.

The immunolocalization of wild-type and mutant $P2X_7$ subunits in transfected cells and the corresponding subcellular distribution profiles show that the translocation of the dominant-negative $P2X_7$ subunits to the plasma membrane is as efficient as the one of wild-type $P2X_7$ subunits. We can conclude from these results that the WC167–168AA or the C168A mutant subunits do not knock-down $P2X_7$ receptor function by intracellular retention or degradation of wild-type subunits. Heteromeric nonfunctional $P2X_7$ receptors composed of wild-type and mutant subunits are translocated to the plasma membrane, so it confirms that the inhibition of $P2X_7$ activity is probably caused by a decrease in the number of homomeric wild-type channels available at the cell surface.

There are 10 conserved cysteines in the ectodomain of P2X receptor family that form disulfide bonds and are important for the correct folding of the ATP binding domain (Clyne et al., 2002). Interestingly, the single mutation C168A was able to mimic the dominant-negative properties of the double mutation WC167–168AA, demonstrating the major contribution of this extracellular cysteine residue to the inhibitory effect and its importance in the normal function of $P2X_7$ receptors. Although not silent, the rat $P2X_2$ C164A and human $P2X_1$ C165A mutant receptors have been shown to be deficient in trafficking to the surface (Clyne et al., 2002; Ennion and Evans, 2002). According to our immunolocalization data, substitution of Cys168 with alanine in $P2X_7$ did not lead to disturbed trafficking of the receptors. However, the loss of a disulfide bridge could explain the inhibitory effect of the mutation through a major conformational change in the

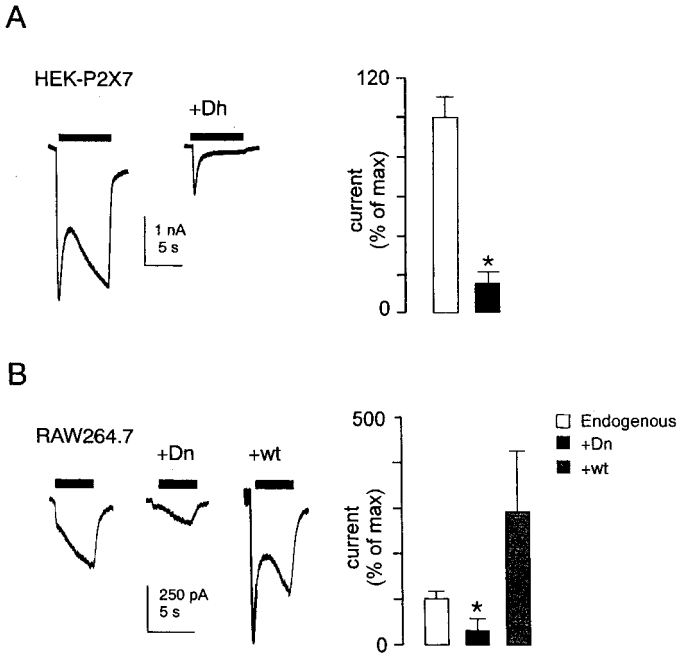

Fig. 7. Suppression of endogenous $P2X_7$ receptor currents by dominant-negative subunits. A, decreased current responses to application of 700 μM BzATP in HEK293-$P2X_7$ cells transfected with the WC167–168AA mutant subunit. B, inhibition of BzATP-induced currents in RAW 264.7 macrophage cell line transfected with the C168A mutant subunit. Cells transfected with wild-type $P2X_7$ subunits produced larger currents in response to BzATP.

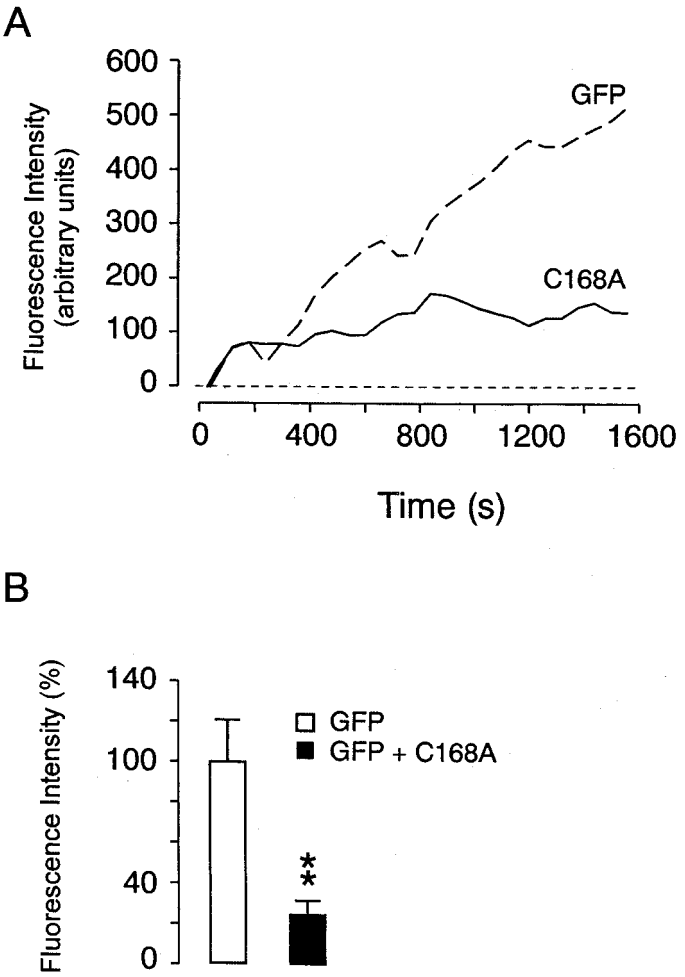

Fig. 8. Inhibition of pore formation in RAW264.7 cells by dominant-negative subunits. A, time-dependent increase in fluorescence intensity in response to application of 3 mM ATP is suppressed by the transient expression of C168A mutant subunit in RAW264.7 cells. GFP indicates cells that were transfected with empty vector (see *Materials and Methods*). Agonist was added at time 0 s. B, normalized average fluorescence intensities in response to 30-min agonist stimulation in RAW264.7 cells transfected with GFP alone or with C168A mutant constructs.

ATP binding domain or other critical domains of the receptor-channel.

In cells coexpressing the wild-type and the mutant subunits, the relative proportion of functional homomeric wild-type, silent homomeric mutant, and silent or functionally impaired heteromeric $P2X_7$ receptors follows a statistical distribution that depends on the ratio of the subunits, on the affinity of the intersubunit associations, and on the number of subunits in the ion channel. If the affinity for intersubunit association is similar between mutant and wild-type subunits and one single subunit is necessary and sufficient to block a $P2X_7$ channel, the binomial distribution of the different populations of receptors would translate into an exponential decrease in $P2X_7$ current with increasing proportions of mutant subunits (Table 2).

Indeed, the experimental dose-response curves for the dominant-negative effects are clearly exponential and are compatible with a trimeric or tetrameric configuration of $P2X_7$ receptors (Table 2). These data support a model in which one dominant-negative subunit is sufficient to knock down the function of the channel. Therefore, it provides further evidence that the inhibitory effect of these dominant-negative subunits is not merely an effect of dilution of functional subunits. P2X channels are believed to have a trimeric architecture (Nicke et al., 1998), so in native preparations, the cotranslation of only one dominant-negative mutant subunit with two wild-type endogenous subunits might generate a significant knock-down of $P2X_7$ responses (Table 2).

When we tested the effectiveness of the dominant-negative mutant $P2X_7$ subunits on a pre-existing pool of $P2X_7$ receptors in a HEK293 stable cell line, we recorded a significant reduction of BzATP-induced $P2X_7$ currents. As a proof-of-concept validating this selective dominant-negative approach, transient expression of mutant subunits in natively $P2X_7$-expressing RAW264.7 cells also led to a significant knock-down of endogenous $P2X_7$ receptor function. However, we noticed that in both cases, the decrease of current was lower than that observed in our cotransfection experiments. The simplest interpretation of this apparently lower inhibition in native preparations would be that the amount of cotranslation of mutant subunits with de novo wild-type $P2X_7$ subunits is limited by the short time window of transient expression. The turnover rate of $P2X_7$ receptors in RAW264.7 cells is not known, but half-lives as long as 10 days have been reported for other ionotropic receptors (Wang et al., 1999). Longer-term coexpression of mutant subunits with endogenous $P2X_7$ subunits is likely to improve the effectiveness of this dominant-negative approach in macrophage-related cell types. Because these cell types are notoriously resistant to transfection (Burke et al., 2002), transgenic or viral expression of dominant-negative WC167–168AA or C168A mutant $P2X_7$ subunits would provide more effective approaches to knock down native $P2X_7$ responses in peripheral macrophages and in microglia.

In conclusion, dominant-negative $P2X_7$ subunits can be used to selectively suppress the channel activity of $P2X_7$ receptors and the associated pore formation without interfering with a wide variety of other conductances sensitive to extracellular ATP. Thus, they provide novel genetic tools to investigate the physiological and pathological role of native PX_7 receptors in inflammation and in immune response.

Acknowledgments

We thank David Elliot (AstraZeneca) and Marie-France Witty for technical assistance and Dr. Ariel Ase for help with confocal microscopy as well as helpful discussions.

References

Ballerini P, Rathbone MP, Di Iorio P, Renzetti A, Giuliani P, D'Alimonte I, Trubiani O, Caciagli F, and Ciccarelli R (1996) Rat astroglial P2Z (P2X7) receptors regulate intracellular calcium and purine release. *Neuroreport* **7:**2533–2537.

Bianchi BR, Lynch KJ, Touma E, Niforatos W, Burgard EC, Alexander KM, Park HS, Yu H, Metzger R, Kowaluk E, et al. (1999) Pharmacological characterization of recombinant human and rat P2X receptor subtypes. *Eur J Pharmacol* **376:**127–138.

Boué-Grabot E, Akimenko MA, and Séguéla P (2000a) Unique functional properties of a sensory neuronal P2X ATP-gated channel from zebrafish. *J Neurochem* **75:**1600–1607.

Boué-Grabot E, Archambault V, and Séguéla P (2000b) A protein kinase C site highly conserved in P2X subunits controls the desensitization kinetics of P2X(2) ATP-gated channels. *J Biol Chem* **275:**10190–5.

Buell G, Chessell IP, Michel AD, Collo G, Salazzo M, Herren S, Gretener D, Grahames C, Kaur R, Kosco-Vilbois MH, et al. (1998) Blockade of human P2X7 receptor function with a monoclonal antibody. *Blood* **92:**3521–3528.

Burke B, Sumner S, Maitland N, and Lewis CE (2002) Macrophages in gene therapy: cellular delivery vehicles and in vivo targets. *J Leukoc Biol* **72:**417–428.

Chakfe Y, Séguin R, Antel JP, Morissette C, Malo D, Henderson D, and Séguéla P (2002) ADP and AMP induce interleukin-1beta release from microglial cells through activation of ATP-primed P2X7 receptor channels. *J Neurosci* **22:**3061–3069.

Chessell IP, Michel AD, and Humphrey PP (1998) Effects of antagonists at the human recombinant P2X7 receptor. *Br J Pharmacol* **124:**1314–1320.

Chiozzi P, Sanz JM, Ferrari D, Falzoni S, Aleotti A, Buell GN, Collo G, and Di Virgilio F (1997) Spontaneous cell fusion in macrophage cultures expressing high levels of the P2Z/P2X7 receptor. *J Cell Biol* **138:**697–706.

Clyne JD, Wang LF, and Hume RI (2002) Mutational analysis of the conserved cysteines of the rat P2X2 purinoceptor. *J Neurosci* **22:**3873–3880.

Collo G, Neidhart S, Kawashima E, Kosco-Vilbois M, North RA, and Buell G (1997) Tissue distribution of the P2X7 receptor. *Neuropharmacology* **36:**1277–1283.

Cucchiarini M, Ren XL, Perides G, and Terwilliger EF (2003) Selective gene expression in brain microglia mediated via adeno-associated virus type 2 and type 5 vectors. *Gene Ther* **10:**657–667.

Di Virgilio F, Chiozzi P, Falzoni S, Ferrari D, Sanz JM, Venketaraman V, and Baricordi OR (1998) Cytolytic P2X purinoceptors. *Cell Death Differ* **5:**191–199.

Duan S, Anderson CM, Keung EC, Chen Y, and Swanson RA (2003) P2X7 receptor-mediated release of excitatory amino acids from astrocytes. *J Neurosci* **23:**1320–1328.

Dubyak GR and el-Moatassim C (1993) Signal transduction via P2-purinergic receptors for extracellular ATP and other nucleotides. *Am J Physiol* **265:**C577–C606.

el-Moatassim C and Dubyak GR (1993) Dissociation of the pore-forming and phospholipase D activities stimulated via P2z purinergic receptors in BAC1.2F5 macrophages. Product inhibition of phospholipase D enzyme activity. *J Biol Chem* **268:**15571–15578.

Ennion SJ and Evans RJ (2002) Conserved cysteine residues in the extracellular loop of the human P2X(1) receptor form disulfide bonds and are involved in receptor trafficking to the cell surface. *Mol Pharmacol* **61:**303–311.

Evans RJ, Lewis C, Buell G, Valera S, North RA, and Surprenant A (1995) Pharmacological characterization of heterologously expressed ATP-gated cation channels (P2x purinoceptors). *Mol Pharmacol* **48:**178–183.

Ferrari D, Stroh C, and Schulze-Osthoff K (1999) P2X7/P2Z purinoreceptor-mediated activation of transcription factor NFAT in microglial cells. *J Biol Chem* **274:**13205–10.

Ferrari D, Wesselborg S, Bauer MK, and Schulze-Osthoff K (1997) Extracellular ATP activates transcription factor NF-kappaB through the P2Z purinoreceptor by selectively targeting NF-kappaB p65. *J Cell Biol* **139:**1635–1643.

Humphreys BD, Virginio C, Surprenant A, Rice J, and Dubyak GR (1998) Isoquinolines as antagonists of the P2X7 nucleotide receptor: high selectivity for the human versus rat receptor homologues. *Mol Pharmacol* **54:**22–32.

Jiang LH, Mackenzie AB, North RA, and Surprenant A (2000a) Brilliant blue G selectively blocks ATP-gated rat $P2X_7$ receptors. *Mol Pharmacol* **58:**82–88.

Jiang LH, Rassendren F, Surprenant A, and North RA (2000b) Identification of amino acid residues contributing to the ATP-binding site of a purinergic P2X receptor. *J Biol Chem* **275:**34190–34196.

Khakh BS, Bao XR, Labarca C, and Lester HA (1999) Neuronal P2X transmitter-gated cation channels change their ion selectivity in seconds. *Nat Neurosci* **2:**322–330.

Khakh BS, Burnstock G, Kennedy C, King BF, North RA, Séguéla P, Voigt M, and Humphrey PP (2001) International union of pharmacology. XXIV. Current status of the nomenclature and properties of P2X receptors and their subunits. *Pharmacol Rev* **53:**107–118.

Lammas DA, Stober C, Harvey CJ, Kendrick N, Panchalingam S, and Kumararatne DS (1997) ATP-induced killing of mycobacteria by human macrophages is mediated by purinergic P2Z(P2X7) receptors. *Immunity* **7:**433–444.

Le KT, Babinski K, and Séguéla P (1998) Central P2X4 and P2X6 channel subunits coassemble into a novel heteromeric ATP receptor. *J Neurosci* **18:**7152–7159.

MacKenzie A, Wilson HL, Kiss-Toth E, Dower SK, North RA, and Surprenant A (2001) Rapid secretion of interleukin-1beta by microvesicle shedding. *Immunity* **15:**825–835.

Neary JT, Kang Y, Willoughby KA, and Ellis EF (2003) Activation of extracellular

signal-regulated kinase by stretch-induced injury in astrocytes involves extracellular ATP and P2 purinergic receptors. *J Neurosci* **23:**2348–2356.
Nicke A, Baumert HG, Rettinger J, Eichele A, Lambrecht G, Mutschler E, and Schmalzing G (1998) P2X1 and P2X3 receptors form stable trimers: a novel structural motif of ligand-gated ion channels. *EMBO (Eur Mol Biol Organ) J* **17:**3016–3028.
North RA (2002) Molecular physiology of P2X receptors. *Physiol Rev* **82:**1013–1067.
Smith RA, Alvarez AJ, and Estes DM (2001) The P2X7 purinergic receptor on bovine macrophages mediates mycobacterial death. *Vet Immunol Immunopathol* **78:**249–262.
Solle M, Labasi J, Perregaux DG, Stam E, Petrushova N, Koller BH, Griffiths RJ, and Gabel CA (2001) Altered cytokine production in mice lacking $P2X_7$ receptors. *J Biol Chem* **276:**125–132.
Surprenant A, Rassendren F, Kawashima E, North RA, and Buell G (1996) The cytolytic P2Z receptor for extracellular ATP identified as a P2X receptor (P2X7). *Science (Wash DC)* **272:**735–738.
Torres GE, Egan TM, and Voigt MM (1999) Hetero-oligomeric assembly of P2X receptor subunits. Specificities exist with regard to possible partners. *J Biol Chem* **274:**6653–6659.
Virginio C, Church D, North RA, and Surprenant A (1997) Effects of divalent cations, protons and calmidazolium at the rat P2X7 receptor. *Neuropharmacology* **36:**1285–1294.
Virginio C, MacKenzie A, North RA, and Surprenant A (1999a) Kinetics of cell lysis, dye uptake and permeability changes in cells expressing the rat P2X7 receptor. *J Physiol* **519:**335–346.
Virginio C, MacKenzie A, Rassendren FA, North RA, and Surprenant A (1999b) Pore dilation of neuronal P2X receptor channels. *Nat Neurosci* **2:**315–321.
Wang ZZ, Mathias A, Gautam M, and Hall ZW (1999) Metabolic stabilization of muscle nicotinic acetylcholine receptor by rapsyn. *J Neurosci* **19:**1998–2007.

Address correspondence to: Dr. Philippe Séguéla, Montreal Neurological Institute, 3801 University Street, Suite 778, Montreal, QC, Canada, H3A 2B4. E-mail: philippe.seguela@mcgill.ca